Earthquake response analysis of an earth dam

Medhat A.Haroun
University of California, Irvine, USA
Essam A.Abdel-Hafiz
Suez Canal University, Port Said, Egypt

ABSTRACT: The seismic behavior of earth dams was analyzed taking into account the interaction of the dam with the reservoir as well as the effects of differential ground motions along its longitudinal axis. The hydrodynamic pressures exerted on dams with sloping faces were employed to evaluate the added mass which was coupled with the shear deformation theory of the dam to obtain its natural frequencies and modes of vibration. The effects of the amplitude and phase differences of the ground motion on the seismic response of the dam were studied by modelling the dam as a two dimensional shear beam whereas the seismic input, applied at the base of the dam, assumed various forms to reflect the variations in amplitude and phase of the ground motion. It was found that the dam response was not affected by the hydrodynamic pressures but it was sensitive to the assumed variations of ground motion along its base.

1 INTRODUCTION

During an earthquake, a dam moves into and away from the water in the reservoir, in addition to its own lateral vibrations. These motions generate hydrodynamic pressures on the upstream face of the dam, and in turn, influence its deformation. It is also expected that the ground excitation at the foundation level of a long dam may have spatial as well as time variations, and such a differential motion may affect the seismic response of the dam.

The first analysis of the reservoir effects on a dam (Westergaard 1933) dealt with the hydrodynamic pressures on the vertical upstream face of a rigid dam by using a series solution of the governing partial differential equation. This paper elicited numerous discussions, the most interesting of which (Von Karman 1933) dealt with the hydrodynamic forces exerted on the dam by the momentum balance method. Although it was mathematically simple, some steps in the analysis were not clear. Housner (1980) offered a rational explanation of the method and employed it to find an approximate expression for the pressure exerted on a rigid dam having a sloping upstream face. The exact values of the hydrodynamic pressures on such a dam were obtained by conformal mapping (Chwang 1978). By the application of the finite element method (Hall 1981), the frequency dependent transfer functions of the hydrodynamic pressures on rigid and flexible earth dams were presented under both horizontal and vertical ground excitations. Although the effects of the flexibility of dams were introduced some twenty years ago (Chopra 1967), most studies dealing with earth dams have assumed that the dam is rigid for the purpose of computing the hydrodynamic effect, if calculated at all.

Recorded motions of earth dams during past small to moderate earthquakes have shown, in both the time and the frequency domains, that a typical dam responds primarily in what appears to be its fundamental mode in the upstream-downstream direction (Abdel-Ghaffar 1978). This is mainly because of the large thickness of the dam relative to its height. The resistance to the upstream-downstream motion is mainly due to shear distortions, and hence, the dominant displacement at all points within the dam is assumed to be in the horizontal upstream-downstream direction. The relative motions between points located along a horizontal straight line passing through the dam thickness are negligibly small. A common procedure for the seismic analysis of a typical dam is to assume that the same ground motion acts simultaneously at

all points of the dam foundation. However, for relatively long structures, this assumption may not be valid and the effect of earthquake induced differential motions at the foundation level becomes a problem of interest. Time and spatial dependent seismic input at different points along the base of a long dam should be estimated taking into account both the propagation and attenuation of seismic waves but such a procedure is still in its infancy.

The objective of the present study was to investigate the effects of the interaction between an earth dam and its reservoir, and the effects of the spatial variations of ground motion on its response.

2 SYSTEM UNDER CONSIDERATION

The dam under consideration is assumed to be a triangular wedge of a base width B situated in a rectangular canyon of a length L and a height H. The sides of the dam are inclined by an angle θ (a slope of α to 2 - horizontal to vertical). A coordinate system (x, y and z) was used as shown in Figure 1. The displacement of the dam in the x-direction, due to shear deformation, is denoted by u(y,z,t).

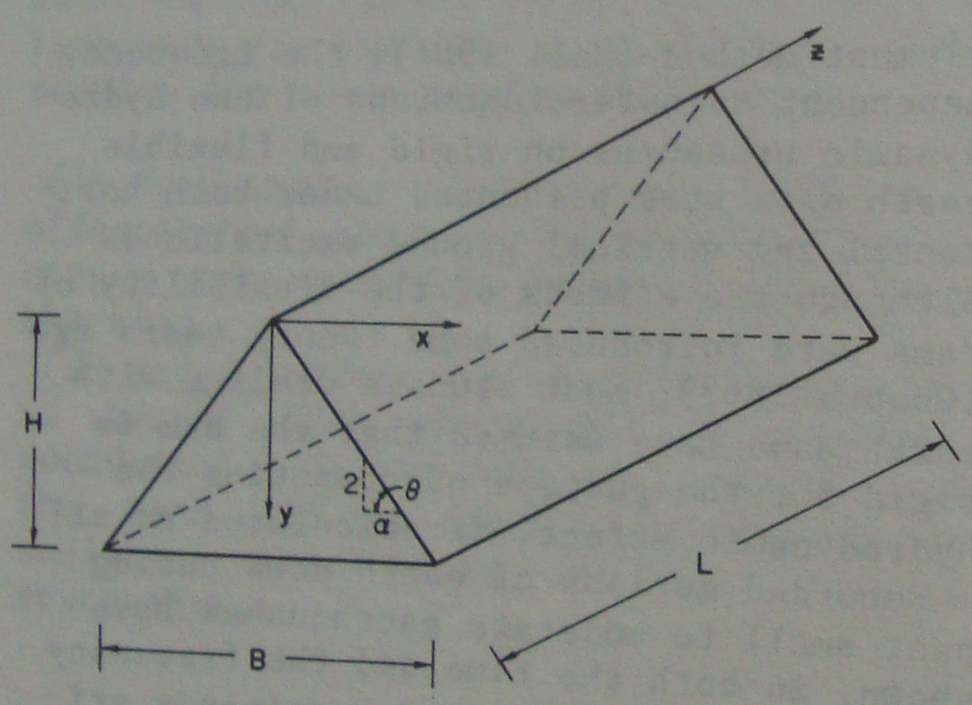

Figure 1. Dam geometry and coordinate system.

3 FINITE ELEMENT MODEL OF THE DAM

In the present analysis, the earth dam was modelled as both one and two dimensional shear beams. Whereas the two dimensional approach was necessary to study the influence of the differential ground motion on the dam response, the one dimension theory was sufficient to study the interaction between a long dam and its reservoir.

It is appropriate, for earth dams consisting of non-cohesive materials, to assume that the average shear modulus varies with the depth from the crest in the form

$$G = \bar{G} \left(\frac{y}{H}\right)^r \tag{1}$$

where $\bar{G}$ is a nominal shear modulus equal to the shear modulus at the base.

The differential equation of motion of a two dimensional shear beam model is

$$\frac{\partial^2 u}{\partial t^2} = \frac{\bar{G}(y/H)^r}{\rho_d}\left(\frac{\partial^2 u}{\partial y^2} + \frac{\partial^2 u}{\partial z^2} + \frac{(r+1)}{y}\frac{\partial u}{\partial y}\right) \tag{2}$$

where ρ_d is the mass density of the dam. This differential equation was transformed to a matrix equation (Haroun 1987) by employing a finite element mesh of the vertical plane of symmetry of the dam as shown in Figure 2. The resulting eigenvalue problem was solved for the dynamic characteristics of the dam.

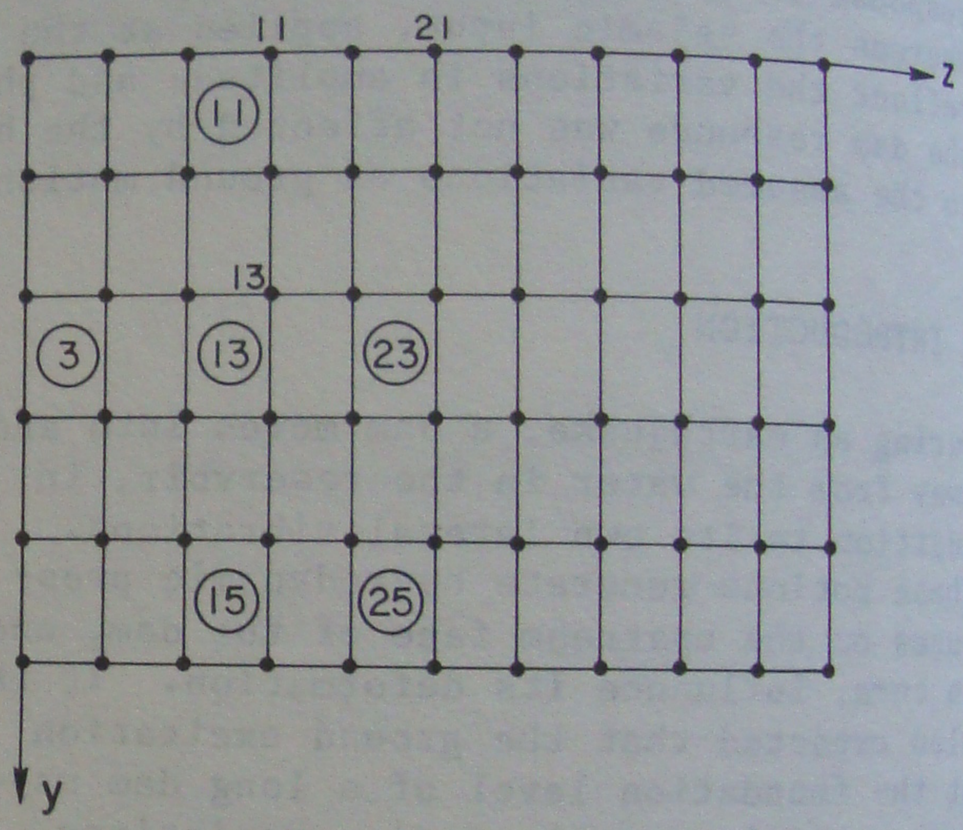

Figure 2. Finite element mesh of the vertical plane of symmetry of the dam.

4 HYDRODYNAMIC PRESSURES ON DAMS WITH SLOPING UPSTREAM FACE

A first step in the analysis of the seismic response of a dam-reservoir system is to calculate the hydrodynamic pressures generated in the fluid domain due to the motions imposed at its boundaries. Fluid domains usually have irregular boundaries of complicated geometries; however, the finite element method offers a simple and accurate procedure to deal with such complexities. Moreover, if it is properly combined with the boundary solution technique, it may even offer a more efficient scheme for the computation of the hydrodynamic pressures (Haroun 1980) on dams with infinite reservoirs.

4.1 Variational Formulation

The variational functional which governs the flow of water in the reservoir can be expressed as

$$J(\phi) = \int_{t_1}^{t_2} \left(-\frac{\rho}{2} \int_{\Omega} (\nabla\phi . \nabla\phi)\, d\Omega + \rho \int_{\Gamma_d} (\phi\, \dot{u}_n)\, d\Gamma \right) dt \qquad (3)$$

where ρ is the mass density of water, Ω is the water domain, Γ is the surface which bounds the reservoir, Γ_d is the interface surface of the reservoir and the dam, and $\dot{u}_n$ is the velocity of the dam normal to the surface Γ_d.

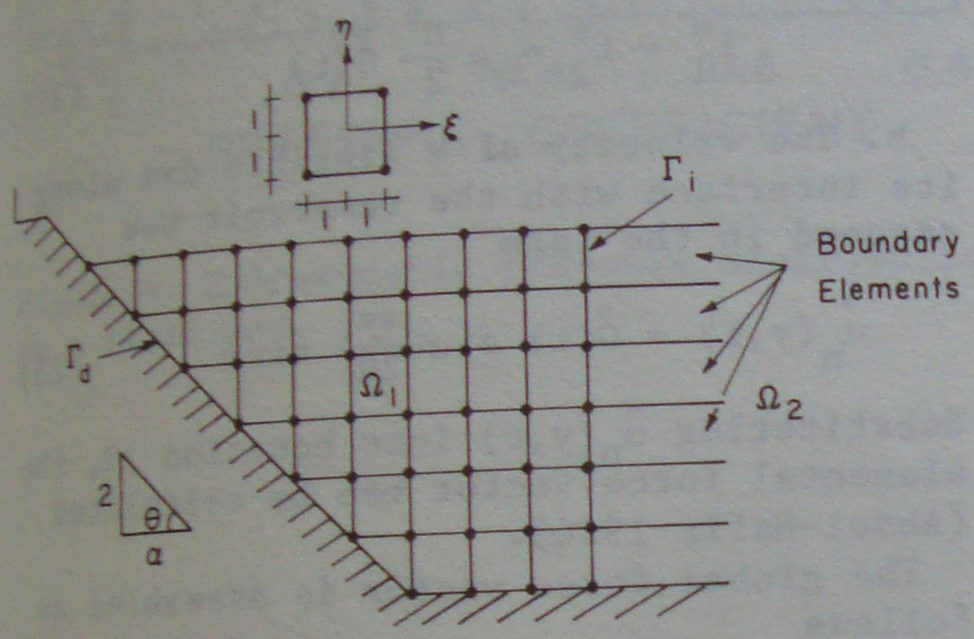

Figure 3. Domain of the reservoir

The finite element method can be used to discretize the fluid domain. The main problem, however, is that the domain Ω is infinite. If one divides it into a finite irregular region near the face of the dam (Ω_1) and an infinite regular region (Ω_2), as shown in Figure 3, then equation 3 can be written in the form

$$J = \int_{t_1}^{t_2} \left(-\frac{\rho}{2} \int_{\Omega_1} (\nabla\phi . \nabla\phi)\, d\Omega - \frac{\rho}{2} \int_{\Omega_2} (\nabla\phi . \nabla\phi)\, d\Omega + \rho \int_{\Gamma_d} (\phi\, \dot{u}_n)\, d\Gamma \right) dt \qquad (4)$$

Each term in equation 4 will be handled by a different procedure.

4.2 Numerical Analysis

The boundary solution technique was applied to the infinite regular region. Using a set of trial functions for ϕ which identically satisfies the Laplace equation in the infinite region, one can replace the volume integral over the region Ω_2 by a surface integral. Applying Green's theorem to the second term of equation 4 yields

$$\frac{\rho}{2} \int_{\Omega_2} (\nabla\phi . \nabla\phi)\, d\Omega = \frac{\rho}{2} \int_{\Gamma_2} \phi \frac{\partial\phi}{\partial n}\, d\Gamma - \int_{\Omega_2} \phi \nabla^2 \phi\, d\Omega = \frac{\rho}{2} \int_{\Gamma_2} \phi \frac{\partial\phi}{\partial n}\, d\Gamma \qquad (5)$$

where Γ_2 is the surface which bounds Ω_2.

A solution for ϕ can be assumed in the form

$$\phi(\bar{x},y,t) = \sum_{i=1}^{I} \overset{*}{N}_i(\bar{x},y)\, A_i(t) \qquad (6)$$

where $\overset{*}{N}_i(\bar{x},y)$ are trial functions which satisfy the Laplace equation, I is the number of trial functions and $(\bar{x},y)$ is a coordinate system with the origin on Γ_i. By choosing the trial functions to satisfy some of the boundary conditions on Γ_2, one can reduce the number of elements on the boundary. An appropriate set of trial functions can be expressed as

$$\overset{*}{N}_i(\bar{x},y) = e^{-\beta_i \bar{x}} \cos\left(\beta_i (H-y)\right);$$

$$\beta_i = (2i-1)\pi/2H \qquad (7)$$

where H is the height of water in the reservoir (full reservoir).

Thus, the integral on the surface Γ_2 can be reduced to one integral only on the interface Γ_i between the region Ω_1 and Ω_2. Assuming the potential function $\bar{\phi}(y,t)$ on Γ_i is given, then equation 7 implies that

$$\bar{\phi}(y,t) = \sum_{i=1}^{I} A_i(t) \cos\left(\beta_i (H-y)\right) \qquad (8)$$

and accordingly (using the orthogonality of the cosine functions)

$$A_i(t) = \frac{2}{H} \int_0^H \bar{\phi}(y,t) \cos\left(\beta_i (H-y)\right) dy \qquad (9)$$

With the aid of the definition of $A_i(t)$, equation 5 yields

$$\frac{\rho}{2} \int_{\Gamma_2} \phi \frac{\partial\phi}{\partial n}\, d\Gamma = \frac{\rho}{H} \sum_{i=1}^{I} \beta_i \left(\int_0^H \bar{\phi}(y,t) \cos\left(\beta_i (H-y)\right) dy \right)^2 \qquad (10)$$

Expressing $\bar{\phi}(y,t)$ in terms of the unknown nodal values of the velocity potential function and of the finite element interpolation functions, one obtains

$$\bar{\phi}(y,t) = \{\tilde{N}\}^T \{\bar{\phi}_{\Gamma_i}\} \tag{11}$$

where $\{\tilde{N}\}$ is the vector of interpolation functions. Thus equation 10 can be rewritten in a matrix form as

$$\frac{\rho}{2} \int_{\Gamma_2} \phi \frac{\partial \phi}{\partial n} d\Gamma = \{\bar{\phi}_{\Gamma_i}\}^T [R_{\Gamma_i}] \{\bar{\phi}_{\Gamma_i}\} \tag{12}$$

in which $\{\bar{\phi}_{\Gamma_i}\}$ is the vector of nodal unknowns along the surface Γ_i, and $[R_{\Gamma_i}]$ is defined as

$$[R_{\Gamma_i}] = \frac{\rho}{H} \sum_{i=1}^{I} \beta_i \{\Psi_{(i)}\}\{\Psi_{(i)}\}^T \tag{13}$$

where

$$\{\Psi_{(i)}\} = \sum_{e=1}^{NEV} \{\psi_{(i)}\}^e \tag{14}$$

and

$$\{\psi_{(i)}\}^e = \frac{H^e}{2} \int_{-1}^{1} \{\tilde{N}\} \cos\beta_i \left(H-\left(\frac{H^e}{2}(2e-1+\eta)\right)\right) d\eta \tag{15}$$

in which H^e is the height of an element, NEV is the total number of elements along Γ_i and e is the element number.

The irregular part of the reservoir was represented by a two dimensional finite element model having both three and four node elements (Figure 3). Each node is assumed to have a one degree of freedom (nodal value of the velocity potential function). The first term in equation 4 leads, after straightforward calculations to

$$\frac{\rho}{2} \int_{\Omega_1} (\nabla\phi . \nabla\phi)\, d\Omega = \{\phi_{\Omega_1}\}^T [R_{\Omega_1}] \{\phi_{\Omega_1}\} \tag{16}$$

For a four node element, the matrix $[R]^e$ can be put in the form

$$[R]^e = \frac{\rho H^e L^e}{12} \begin{bmatrix} 2R_1 & R_2 & -R_1 & R_3 \\ R_2 & 2R_1 & R_3 & -R_1 \\ -R_1 & R_3 & 2R_1 & R_2 \\ R_3 & -R_1 & R_2 & 2R_1 \end{bmatrix} \tag{17}$$

where

$$R_1 = \frac{1}{(L^e)^2} + \frac{1}{(H^e)^2} \tag{18a}$$

$$R_2 = \frac{-2}{(L^e)^2} + \frac{1}{(H^e)^2} \tag{18b}$$

and

$$R_3 = \frac{1}{(L^e)^2} - \frac{2}{(H^e)^2} \tag{18c}$$

in which L^e is the length of the element.

The third term in equation 4 leads to the definition of the force vector. This term can be represented in the form

$$\rho \int_{\Gamma_d} (\phi \dot{u}_n)\, d\Gamma = \{\hat{\phi}_{\Gamma_d}\}^T \{F_{\Gamma_d}\} \tag{19}$$

where $\{\hat{\phi}_{\Gamma_d}\}$ is the vector of unknown nodal values along the dam-reservoir interface, and $\{F_{\Gamma_d}\}$ is the force vector which, in this section, is calculated for two cases:

a. The velocity of a rigid dam along the dam-reservoir interface was assumed as

$$\dot{u}_n(y,t) = \dot{G}(t) \sin\theta \tag{20}$$

The elemental force vector is expressed in terms of the shape functions as

$$\{f\}^e = \rho\dot{G} \int_{-1}^{1} \{\tilde{N}(\eta)\} \frac{ds}{d\eta} \sin\theta\, d\eta \tag{21}$$

where s is an axis oriented along the dam-reservoir interface. Performing the integration, one obtains

$$f_1^e = f_2^e = \rho \frac{H^e}{2} \dot{G}(t) \tag{22}$$

b. The velocity of a flexible dam along its interface with the reservoir was assumed in the form

$$\dot{u}_n(y,t) = \dot{G}(t) \sin\left(\frac{\pi y}{2H}\right) \sin\theta \tag{23}$$

Substituting $\dot{u}_n(y,t)$ into equation 19, the elemental force vector can be calculated (Abdel-Hafiz 1986).

The global force vector is assembled as follows

$$\{F\} = \sum_{e=1}^{NEV} \{f\}^e \tag{24}$$

After substituting equations 12, 16 and 19 into equation 4, the extremization of the variational functional yields the following matrix equation

$$[R]\ \{\phi\} = \{F\} \tag{25}$$

where the matrix [R] includes the contributions of the boundary elements and the finite elements, $\{\phi\}$ represents the vector of unknown nodal values of the velocity potential function and $\{F\}$ is the nodal force vector. Numerical solution of equation 25 provides the values of the velocity potential function which are directly related to the hydrodynamic pressures on the dam.

4.3 Illustrative Example

A computer program was developed to calculate the hydrodynamic pressures on the upstream face of dams. At first, the hydrodynamic pressures on rigid dams with different angles of slopes of the upstream

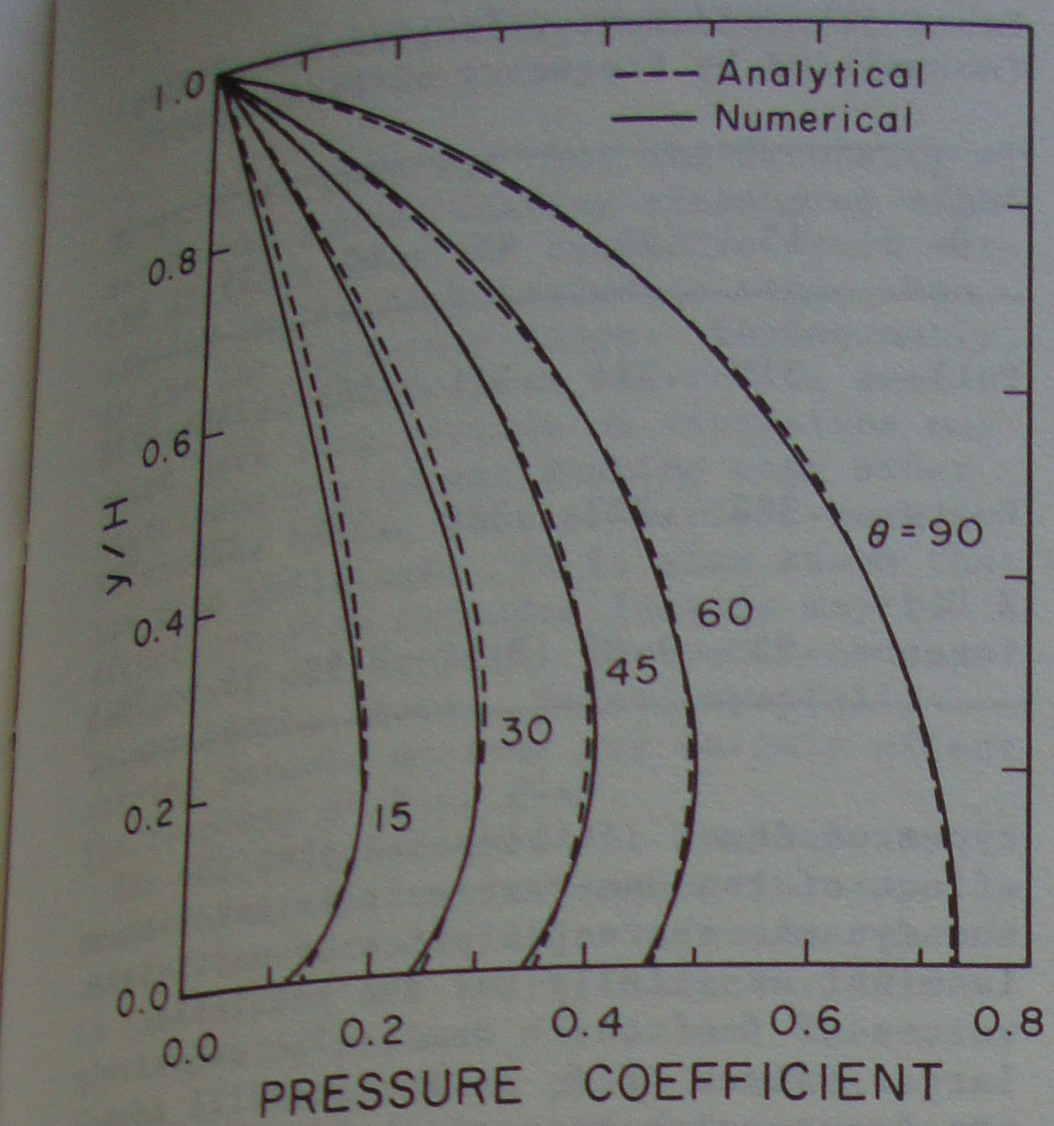

Figure 4. Hydrodynamic pressure distribution on a rigid dam.

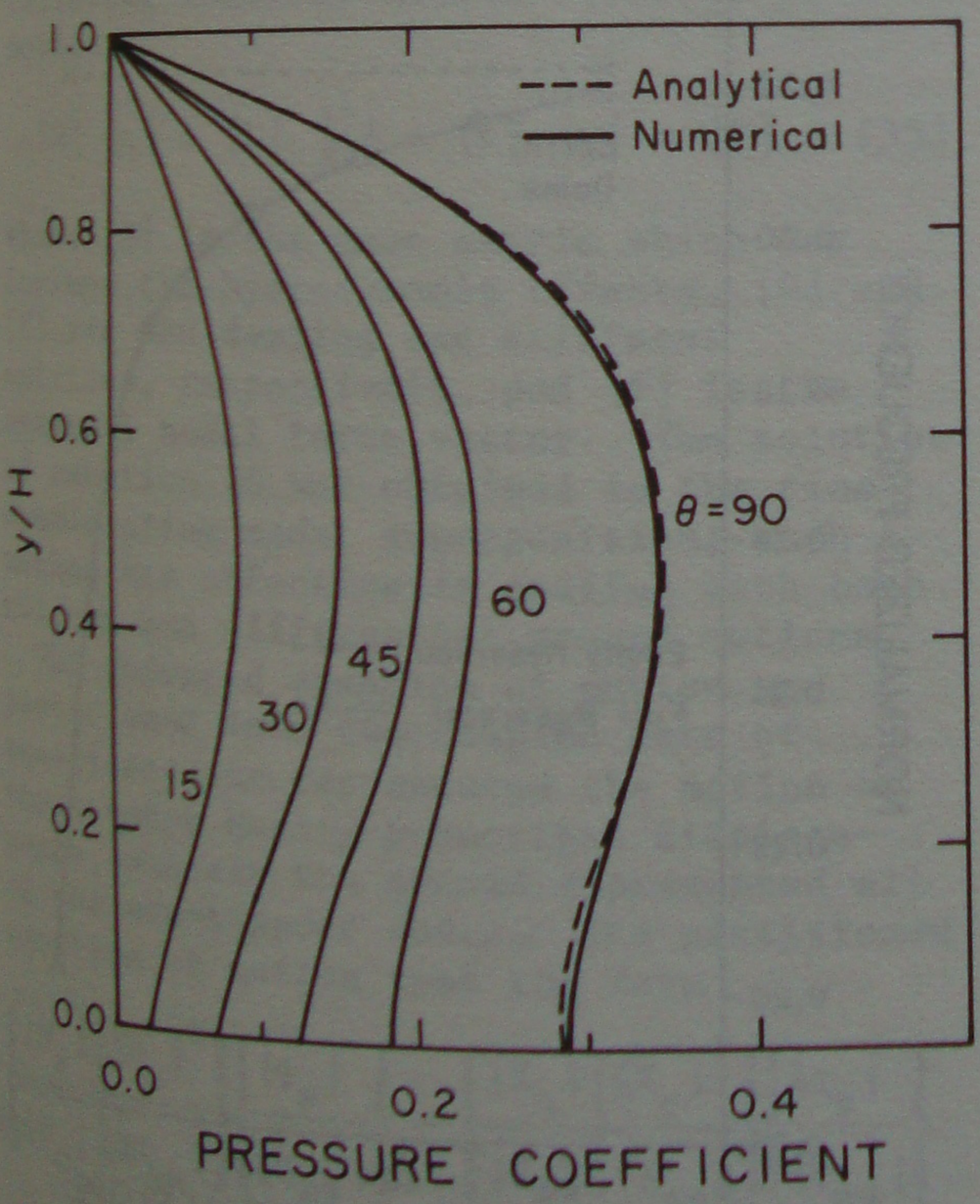

Figure 5. Hydrodynamic pressure distribution on a flexible dam.

face were computed and compared to the exact solution (Chwang 1978). It is clear from Figure 4 that the numerical solution adopted herein is reliable and can be used to predict the pressures on rigid sloping dams with sufficient accuracy. Figure 5 displays the pressure distribution, as calculated from the numerical solution, on a flexible dam for which the deflection was assumed as a sine curve. The exact solution for a dam with a vertical upstream face is also shown for comparison.

5 DAM-RESERVOIR INTERACTION

In the following analysis, a method is developed to make use of the hydrodynamic pressure expressions derived earlier for the derivation of an added mass matrix.

5.1 Hydrodynamic Pressures

The hydrodynamic pressures calculated according to equation 25 represent the pressures at the different nodes of the region Ω_1 including those on the dam-reservoir interface. An equation, similar to equation 25, can be also written for the pressures but in a partitioned form as

$$\begin{bmatrix} [R_i] & [R_c]^T \\ \hline [R_c] & [R_n] \end{bmatrix} \begin{Bmatrix} \{p_i\} \\ \hline \{p_n\} \end{Bmatrix} = \begin{bmatrix} [S_i] \\ \hline [S_c] \end{bmatrix} \{\ddot{q}\} \qquad (26)$$

where $\{\ddot{q}\}$ is the nodal acceleration vector of the dam. The subscripts i and n denote interface and non-interface nodes, respectively, whereas the subscript c refers to the coupling between interface and non-interface nodes.

From equation 26, the equation for the interface nodes is written as

$$[R_i]\{p_i\} + [R_c]^T\{p_n\} = [S_i]\{\ddot{q}\} \qquad (27)$$

whereas the equation of the non-interface nodes is given by

$$[R_c]\{p_i\} + [R_n]\{p_n\} = [S_c]\{\ddot{q}\} \qquad (28)$$

Equation 28 can be solved for the pressure at the non-interface nodes, and upon the substitution in equation 27, one obtains the pressure at the interface nodes

$$\left[[R_i] - [R_c]^T[R_n]^{-1}[R_c]\right]\{p_i\} = \left[[S_i] - [R_c]^T[R_n]^{-1}[S_c]\right]\{\ddot{q}\} \qquad (29)$$

If one defines

$$[R_{eff}] = [R_i] - [R_c]^T[R_n]^{-1}[R_c] \quad (30a)$$

$$[S_{eff}] = [S_i] - [R_c]^T[R_n]^{-1}[S_c] \quad (30b)$$

then the pressure at the interface nodes can be expressed as

$$\{p_i\} = [R_{eff}]^{-1}[S_{eff}]\{\ddot{q}\} \quad (31)$$

Equation (31) offers an expression for the added mass [AM] which is defined by

$$[AM] = [R_{eff}]^{-1}[S_{eff}] \quad (32)$$

The matrix [R] was calculated earlier in section 4.2. The matrix [S] can be also evaluated using the finite element model of the reservoir, and for a four node element, it can be expressed as

$$[S]^e = \frac{\rho H^e L^e}{36}\begin{bmatrix} 4 & 2 & 1 & 2 \\ 2 & 4 & 2 & 1 \\ 1 & 2 & 4 & 2 \\ 2 & 1 & 2 & 4 \end{bmatrix} \quad (33)$$

The order of the added mass matrix is $N_i x N_i$ where N_i is the number of interface nodes excluding the free surface node.

5.2 Illustrative Examples

The method of computation outlined above was used to compute the dynamic characteristics of an earth dam of a height 160 feet, an average shear wave velocity of 1000 ft/sec and a mass density of 4.03 $lb.sec^2/ft^4$.

The dam was modelled as a one dimension shear beam. Such a representation was adequate for the purpose of studying the hydrodynamic effects on the characteristics of the dam. Different angles of upstream slope were assumed. Although some of these values were not practical for earth dams, it was meant to emphasize the effect of the upstream slope on the dam-reservoir interaction. Table 1 presents the normalized fundamental frequencies of dams for different angles of slope of the upstream face (θ). These values were normalized by the fundamental frequency of the reservoir which is given by

$$\omega_{res} = \pi c_w / 2H \quad (34)$$

where c_w denotes the velocity of sound in water. Figure 6 also displays the effects of θ on the normalized fundamental frequencies of vibrations for different types of dams. It is noted that the effect of the dam-reservoir interaction on the dynamic characteristics of earth dams is minor especially for the realistic values of θ of earth dams. For relatively larger values of θ, as for rockfill dams, the frequencies were slightly affected by the hydrodynamic pressure. It is also noted that the hydrodynamic pressures have significant effects on the dynamic characteristics of dams with vertical upstream face such as concrete gravity dams.

Table 1. Fundamental frequencies of dams (normalized by frequency of reservoir)

Angle θ	15	30	45	60	75	90
Full	.319	.316	.311	.303	.288	.198
Empty	.322	.322	.322	.322	.322	.322
% Difference	.93	1.86	3.42	5.90	10.6	38.5

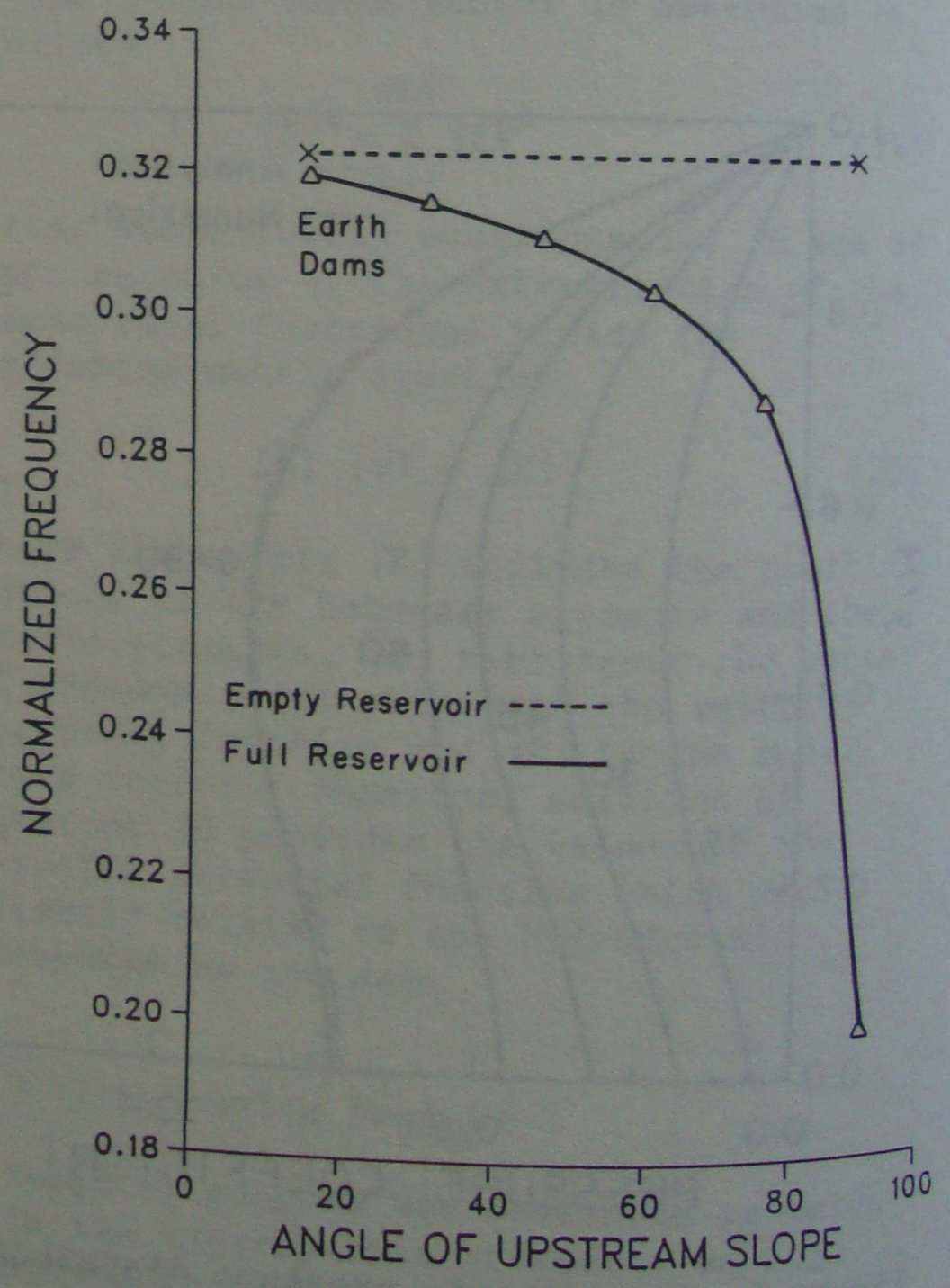

Figure 6. Normalized fundamental frequency.

6 EARTH DAMS SUBJECTED TO DIFFERENTIAL GROUND MOTIONS

It is often observed that the intensity of earthquake ground shaking attenuates with the distance from the causative fault more rapidly in the high frequency range than in the low frequency range. Consequently, at large distances from the fault, dams which have long periods of vibrations may experience a stronger shaking than other structures having shorter periods such as low rise buildings. It is also known that structures with extended lengths may be damaged by differential movements caused by earthquake waves. Hence, spatially varying seismic motions may largely affect the response of long dams.

The following formulation handles any spatial and time variations of the input motion; however, the major problem remains in identifying the appropriate variations of the ground motion. It is not the intent of the study to provide results that can be directly applied in practice but to provide insight into the behavior of dams to some forms of assumed differential ground excitations.

6.1 Matrix Equation of Motion

The linear earthquake response of dams, as many other structures, is governed by the following familiar matrix equation of motion

$$[M]\{\ddot{q}\} + [C]\{\dot{q}\} + [K]\{q\} = \{F\} \quad (35)$$

where [M] is the mass matrix which may include the hydrodynamic effects, [C] and [K] are the damping and stiffness matrices, respectively, and $\{F\}$ is the external nodal force vector. The solution of equation 35 was obtained in the time domain using modal superposition; such a method was effective in dealing with both uniform and differential ground motions.

The undamped equation of motion was partitioned into two coupled sets of equations: one represented the motion of those nodes having prescribed displacements, whereas the second represented all of the non-support nodes. The partitioned equation of motion took the form

$$\left[\begin{array}{c|c} [M_s] & [M_c]^T \\ \hline [M_c] & [M_{ns}] \end{array}\right]\left\{\begin{array}{c} \{\ddot{q}_s\} \\ \hline \{\ddot{q}_{ns}\} \end{array}\right\} + \left[\begin{array}{c|c} [K_s] & [K_c]^T \\ \hline [K_c] & [K_{ns}] \end{array}\right]\left\{\begin{array}{c} \{q_s\} \\ \hline \{q_{ns}\} \end{array}\right\} = \left\{\begin{array}{c} \{F_s\} \\ \hline \{0\} \end{array}\right\} \quad (36)$$

where $\{q_s\}$ and $\{\ddot{q}_s\}$ are the vectors of prescribed support displacements and accelerations, respectively, and $\{q_{ns}\}$ and $\{\ddot{q}_{ns}\}$ are the vectors of non-support displacements and accelerations. The subscripts s and ns denote support and non-support nodes whereas the subscript c is used for the matrices which represent the coupling effects between the support and non-support nodes.

The displacement vector of the non-support nodes can be considered as the sum of two vectors

$$\{q_{ns}\} = \{q_i\} + \{q_d\} \quad (37)$$

where $\{q_i\}$ is a pseudo-static displacement and $\{q_d\}$ is the dynamic displacement. With the aid of equation 37, equation 36 leads to the governing equation for non-support nodes as

$$[M_c]\{\ddot{q}_s\} + [M_{ns}]\{\ddot{q}_i\} + [M_{ns}]\{\ddot{q}_d\} + [K_c]\{q_s\} + [K_{ns}]\{q_i\} + [K_{ns}]\{q_d\} = \{0\} \quad (38)$$

The displacement vector $\{q_i\}$ is defined as a vector which corresponds to no internal strain energy in the dam if it is acted upon by a "static" support displacement of magnitude $\{q_s\}$. This definition implies

$$[K_c]\{q_s\} + [K_{ns}]\{q_i\} = \{0\} \quad (39)$$

and therefore,

$$\{q_i\} = -[K_{ns}]^{-1}[K_c]\{q_s\} \quad (40)$$

Substitution of equation 40 into equation 38 yields

$$[M_{ns}]\{\ddot{q}_d\} + [K_{ns}]\{q_d\} = -\left[[M_c] - [M_{ns}][K_{ns}]^{-1}[K_c]\right]\{\ddot{q}_s\} \quad (41)$$

which can be written more conveniently in the familiar form

$$[M_{ns}]\{\ddot{q}_d\} + [K_{ns}]\{q_d\} = \{F_{eff}\} \quad (42)$$

where the effective force vector $\{F_{eff}\}$ is defined as

$$\{F_{eff}\} = -[M_{eff}]\{\ddot{q}_s\} \quad (43)$$

in which the effective mass matrix is defined as

$$[M_{eff}] = \left[[M_c] - [M_{ns}][K_{ns}]^{-1}[K_c]\right] \quad (44)$$

Thus, equation 42 represents the matrix equation of motion of the non-support

nodes. The effective force vector is dependent on the ground motion specified at each of the support nodes.

6.2 Effective Force Vector

To investigate the effect of a time lag of the input motion at each of the support nodes, two cases were considered as shown in Figure 7.

a. Travelling Waves: An input motion was selected in the form $\sin(2\pi(z-ct)/\lambda)$ which represents a sine wave of a length λ propagating with a speed c. The wave period T can be expressed in terms of the wave length and the propagation speed as

$$T = \lambda/c \tag{45}$$

In this case, the ground motion at any two nodal points of an element along the base of the dam can be expressed as

$$\{\ddot{q}_s\}^{e^T} = \{\ddot{q}^e_1, \ddot{q}^e_2\} \tag{46}$$

where $$\ddot{q}^e_2(t) = \ddot{q}^e_1\left(2\pi(t-L^e/c)/\lambda\right) \tag{47}$$

in which L^e is the separation distance between the two nodes, i.e., the length of the element.

b. Time-delayed Earthquake Motion: In this case, the ground motion at any two nodal points of an element along the base was given by equation 46 but

$$\ddot{q}^e_2(t+\Delta\hat{t}) = \ddot{q}^e_1(t) \tag{48}$$

in which $\Delta\hat{t}$ is an assumed time lag of the earthquake record.

It should be noted that the ground acceleration vector, in contrary to the case of uniform ground motion, is no longer proportional to a specific time dependent function. The vector $\{\ddot{q}_s\}$ must be computed at each time step. Such input excites both the symmetric and asymmetric modes of the dam.

Following the standard steps in a normal mode analysis, and employing the orthogonality conditions, one can reduce the mass and the stiffness matrices to diagonal forms. In a standard analysis, the generalized load is proportional to the amplitude of the ground acceleration by a constant modal participation factor. This is not true for the type of excitation described herein where the generalized load has to be computed at each time step.

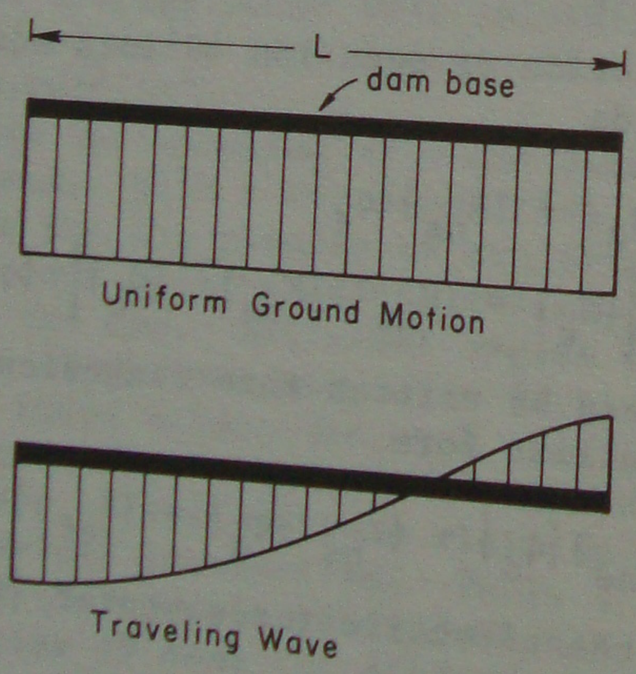

Figure 7. Variation of input motion at the base of the dam.

6.3 Illustrative Examples

A computer program was developed to investigate the effects of amplitude and phase difference of the ground motion on the dynamic response of dams having different length to height ratios. The properties of the dam were chosen as those given earlier whereas the shear modulus was assumed to vary in proportion to the cubic root of the depth measured from the dam crest. It should be noted that the ratio L/H in the following examples reflects primarily the value of the dam length since the height of the dam was taken constant at 160 feet. A viscous damping ratio in the dam body was assumed to be 5 percent of the critical damping.

A parametric study of the effects of the propagation speeds and the periods of travelling waves on the response was conducted. Figure 8 shows the maximum displacements at node number 21 due to individual seismic waves propagating at speeds ranging from 4000 to 8000 ft/sec for a (L/H) ratio of 5. The periods of the waves were assumed to vary between 0.2 to 0.5 seconds yielding a wide range for the values of the wave length between 800 to 4000 feet. The limiting case for $c = \infty$ is also shown in the figure. It was found that, for the same L/H ratio, the displacement was appreciably affected by the change in the period while its dependence on the propagation speed was little pronounced except near resonance. It is noted that the dam response due to the travelling waves can be magnified

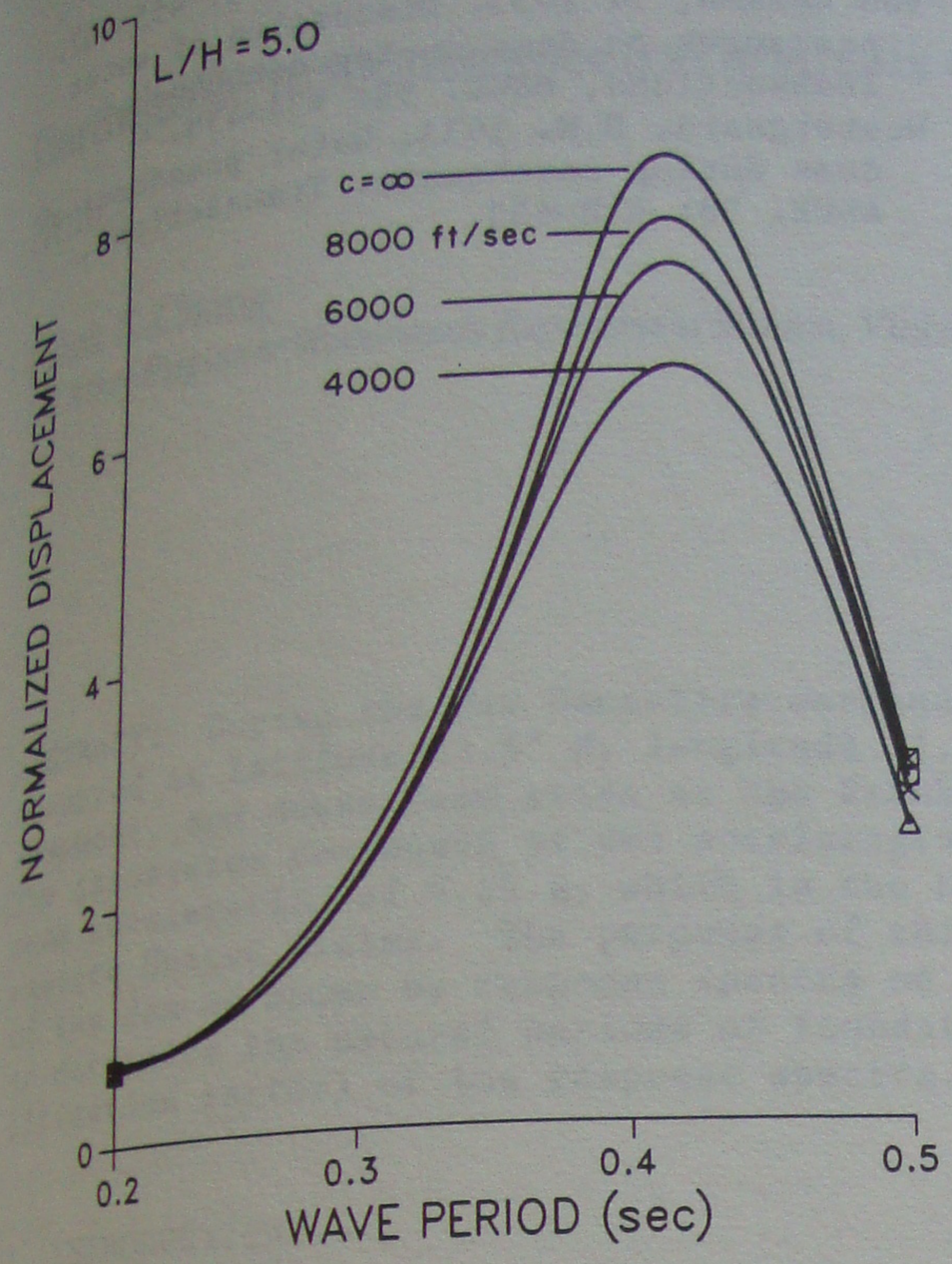

Figure 8. Maximum displacement due to a traveling wave.

considerably if the wave period is equal to or near the fundamental period of the dam.

The component of the 1940 El Centro earthquake was applied at the base of the dam with a time shift of 0.02 seconds. Figure 9 shows the time history of the displacement at node number 21 for a value of L/H = 5 whereas Figure 10 presents a plot of the maximum response at nodes 11 and 21 for uniform and time-delayed earthquake motions versus L/H ratio. It is clear in this case that the response due to a uniform excitation exceeds the response due to a phased ground motion.

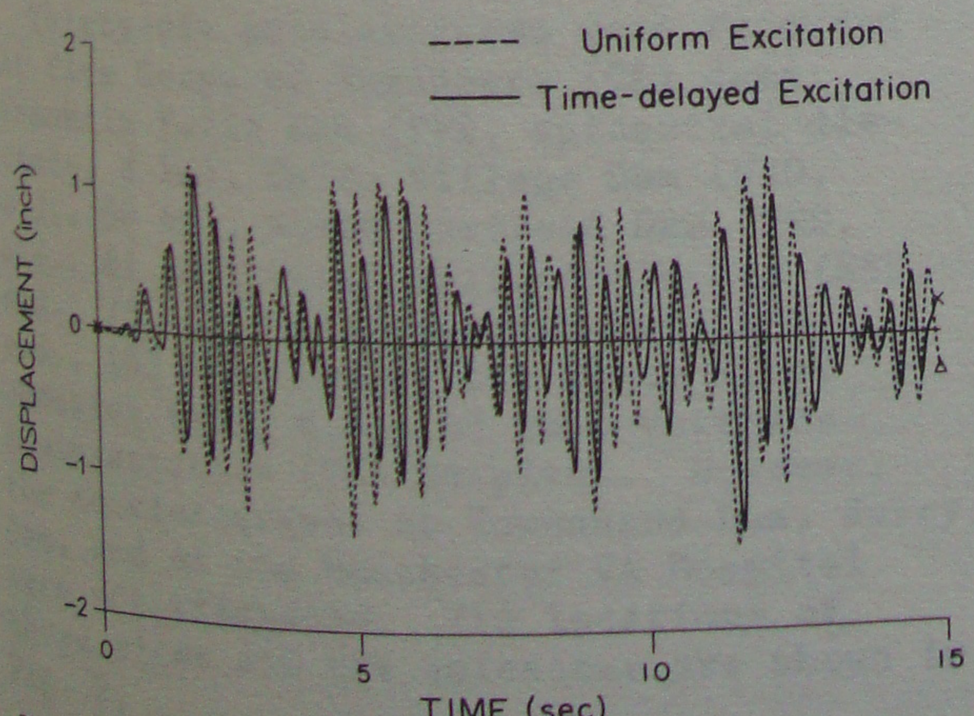

Figure 9. Time history of displacement at node 21 due to a time-delayed excitation.

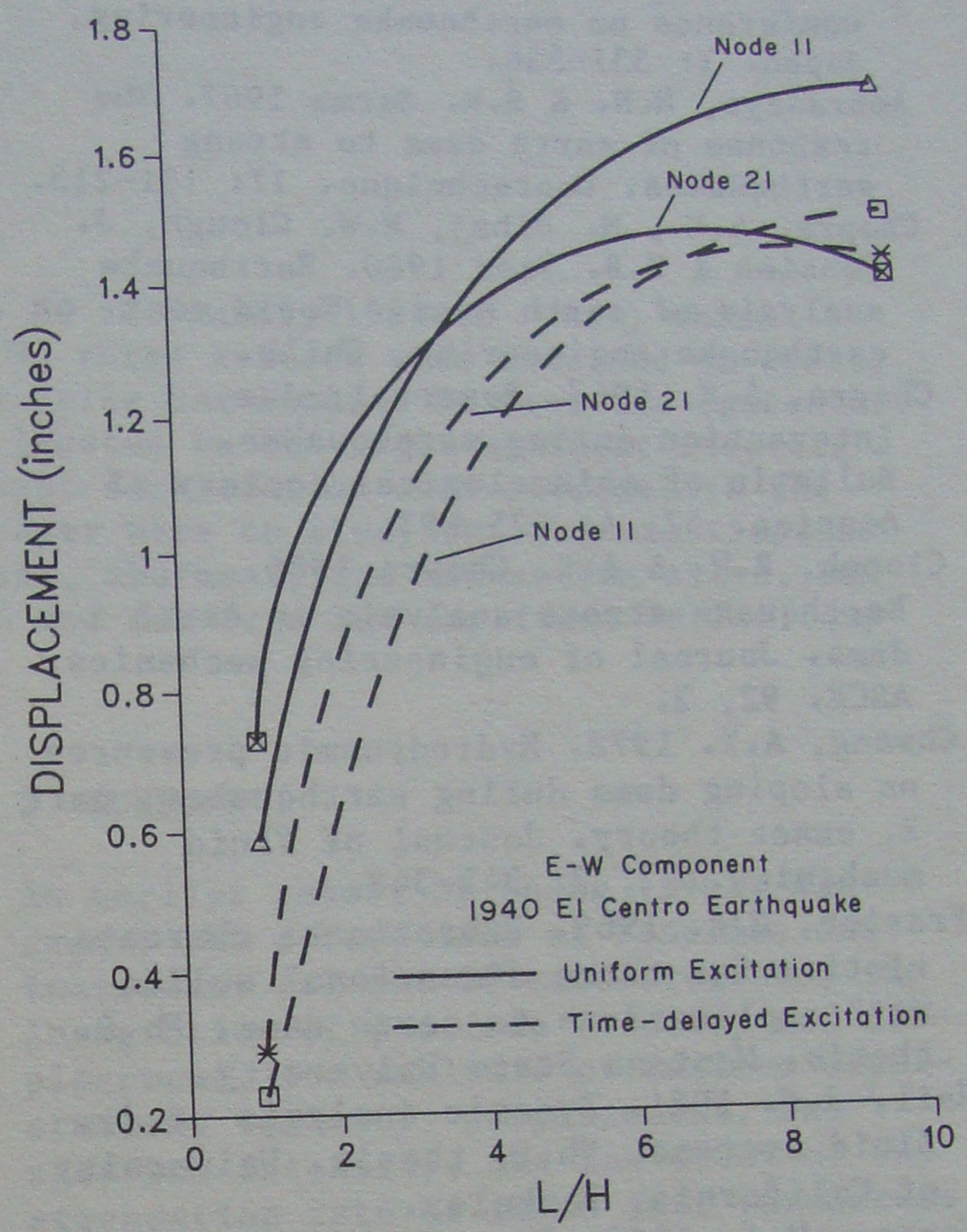

Figure 10. Maximum displacement due to a time-delayed excitation.

7 CONCLUSIONS

The seismic behavior of earth dams was analyzed taking into account the interaction of the dam with the reservoir as well as the effects of differential ground motions along its longitudinal axis. It was found that the dam response was not affected by the hydrodynamic pressures but it was sensitive to the assumed variations of ground motion along its base.

8 REFERENCES

Abdel-Ghaffar, A.M. & R.F. Scott 1978. An investigation of the dynamic characteristics of an earth dam. Report EERL 78-02. California Institute of Technology, Pasadena.

Abdel-Ghaffar, A.M. & R.F. Scott 1979. Experimental investigation of the dynamic response characteristics of an earth dam. U.S. national conference on earthquake engineering, Stanford.
Abdel-Hafiz, E.A. 1986. Seismic analysis of fluid-structure systems. Ph.D. thesis. Univ. of California, Irvine.
Ambraseys, N.N. 1960. On the seismic behavior of earth dams. Second world conference on earthquake engineering, Japan. I: 331-356.
Ambraseys, N.N. & S.K. Sarma 1967. The response of earth dams to strong earthquakes. Geotechnique. 17: 181-213.
Chopra, A.K., M. Dibaj, R.W. Clough, J. Penzien & H.B. Seed 1960. Earthquake analysis of earth dams. World conf. on earthquake engineering, Chile.
Chopra, A.K. 1967. Reservoir-dam interaction during earthquakes. Bulletin of seismological society of America. 57, 4: 675-687.
Clough, R.W. & A.K. Chopra 1966. Earthquake stress analysis in earth dams. Journal of engineering mechanics, ASCE. 92, 2.
Chwang, A.T. 1978. Hydrodynamic pressures on sloping dams during earthquakes, part 2, exact theory. Journal of fluid mechanics. 87, 2: 343-348.
Frazier, G.A. 1969. Vibrational characteristics for three-dimensional solids with applications to earth dams. Ph.D. thesis. Montana State University.
Hall, J.F. 1981. Dynamic analysis of dam-fluid systems. Ph.D. thesis. University of California, Berkeley.
Haroun, M.A. 1980. Dynamic analyses of liquid storage tanks. EERL 80-04, California Inst. of Tech., Pasadena.
Haroun, M.A. & E.A. Abdel-Hafiz 1987. Seismic response analysis of earth dams under differential ground motion. Seism. society of America (in press).
Housner, G.W. 1980. The momentum-balance method in earthquake engineering. Mechanics today. 5: 113-127.
Loh, C.H. 1985. Analysis of the spatial variation of seismic waves and ground movements from SMART-1 array data. Earthquake engineering and structural dynamics. 13: 561-581.
Martin, G.R. 1965. The response of earth dams to earthquakes. Ph.D. thesis. University of California, Berkeley.
Newmark, N.M. 1967. Problems in wave propagation in soil and rock. Symposium on wave propagation & dynamic properties of earth materials, Albuquerque: 7-26.
O'Rourke, M.J., G. Castro & N. Centola 1980. Effects of seismic wave Propagation upon buried pipelines. Earthquake eng. & structural dynamics. 8: 455-467.
Von Karman, T. 1933. Discussion of water pressures on dams during earthquake. Transactions, ASCE. 98: 434-436.
Westergaard, H.M. 1933. Water pressures on dams during earthquake. Transactions, ASCE. 98: 418-433.